**V. A. Romaka,** *doc. techn sciences, professor*[1]
**Yu. V. Stadnyk,** *cand. chem. of science*[2]
**L. P. Romaka,** *cand. chem. of science*[2]
**Yu. O. Plevachuk** *doc. phys. and math sciences* [2]
**V. V. Romaka,** *doc. techn sciences,*
*cand. chem. of science, professor* [3]
**A. M. Horyn,** *cand. chem. of science*[2]
**V. Z. Pashkevych,** *cand. tehn. of science*[1]
**A. V. Zelinskiy** *cand. tehn. of science*[2]

[1]National University "Lvivska Politechnika", 12, S.
Bandera Str., Lviv, 79013, Ukraine,
*e-mail: vromaka@polynet.lviv.ua;*
[2]Ivan Franko National University of Lviv, 6,
Kyryla and Mefodiya Str., Lviv, 79005, Ukraine,
*e-mail: lyubov.romaka@lnu.edu.ua*
[3]Leibniz Institute for Solid State and Materials Research,
IFW-Dresden, Helmholtzstr. 20, 01069 Dresden, Germany

# RESEARCH OF THE THERMOELECTRIC MATERIAL $Lu_{1-x}V_xNiSb$: MODELING OF PROPERTIES

*The result of modeling the crystal and electronic structures, thermodynamic and kinetic properties of $Lu_{1-x}V_xNiSb$ is establishing the nature of the generated energy states. It is shown that the semiconductor solid solution $Lu_{1-x}V_xNiSb$ is a promising thermoelectric material, and at a temperature of T≈620 K and a concentration of $Lu_{0.99}V_{0.01}NiSb$, the thermoelectric factor Z values reach the maximum values of ZT = 0.62. It was established that the impurity atoms of V ($3d^34s^2$), introduced into the structure of the LuNiSb compound, simultaneously occupy the crystallographic positions 4a of Lu atoms ($5d^16s^2$) and 4c of Ni atoms ($3d^84s^2$) in different ratios, generating in the band gap $\varepsilon_g$ impurity donor $\varepsilon_D^V$ and acceptor $\varepsilon_A^{Ni}$ energy states. The ratio of concentrations of donors and acceptors determines the location of the Fermi level $\varepsilon_F$ and the mechanisms of electrical conductivity. Bibl. 28, Fig. 6.*

**Key words:** electronic structure, figure of merit of thermoelectric material, resistivity, thermopower coefficient

## Introduction

One of the most studied thermoelectric materials, which have a high efficiency of converting thermal energy into electrical energy, are semiconductor solid substitution solutions based on half-

Heusler phases, in particular, *MNiSn* (*M – Ti, Zr, Hf*) and *RNiSb* (*R – Y, Gd– Lu*) [1, 2], which crystallize in the *MgAgAs* structural type (space group $F\bar{4}3m$ ) [3]. Therefore, one of the subjects of the research presented below is the modeling of the thermodynamic, structural, energy and kinetic properties of the semiconductor thermoelectric material $Lu_{1-x}V_xNiSb$, obtained by doping the base semiconductor *p-LuNiSb* with *V* atoms ($3d^3 4s^2$), introduced into the structure by replacing *Lu* atoms in the 4*a* position ($5d^1 6s^2$). Modeling of the dynamics of the crystal and electronic structures, thermodynamic and kinetic properties of the $Lu_{1-x}V_xNiSb$ semiconductor will allow us to understand the mechanism of generation in the band gap $\varepsilon_g$ of energy states that determine its properties. In practice, this is realized by choosing alloying conditions: the type and concentration of the impurity, the method of introduction, and modes of homogenizing annealing. This is the essence of optimizing the values of the specific electrical conductivity $\sigma(T)$, thermopower coefficient $\alpha(T)$ and thermal conductivity $\kappa(T)$ to the values that will meet the conditions for obtaining the maximum values of the thermoelectric factor Z ($Z = \alpha^2 \cdot \sigma/\kappa$) [2 , 4].

Semiconductor materials, unlike metals or metal alloys, are convenient for optimizing their characteristics and obtaining maximum values of thermoelectric factor. The fact is that in metals and metal alloys, the values of thermopower coefficient $\alpha(T)$ are small, and changes in the values of the coefficient of thermal conductivity $\kappa(T)$ and specific electrical conductivity $\sigma(T)$ due to the constancy of the Lorentz number cannot significantly change the value of the thermoelectric factor *Z*. That is why the optimization of the characteristics by the appropriate doping of semiconductors allows to achieve the conditions under which the values of the thermoelectric factor *Z* will be maximum [4].

In this context, it is extremely important to understand the structural features of the *p-LuNiSb* base semiconductor. Since the optimization of characteristics is carried out by doping *p-LuNiSb*, in order to achieve the maximum efficiency of the conversion of thermal energy into electrical energy, it is necessary to choose the type and concentration of the impurity when the Fermi level $\varepsilon_F$ approaches the zone of continuous energies [2, 4]. And this cannot be done without comprehensive knowledge of the crystal and electronic structures of a semiconductor and their transformation during doping.

The study of the structural, kinetic, and magnetic properties of compounds of half-Heusler phases *RNiSb* (*R – Y, Gd–Lu*) [5, 6] established that their crystal structure is unordered. In addition, it was shown that *RNiSb* compounds are semiconductors and holes are the main current carriers at all investigated temperatures. A detailed analysis of the crystal and electronic structures of half-Heusler *RNiSb* phases allowed the authors of [7] to establish the nature of disorder in their structure. It was shown that there are vacancies (Vac) in crystallographic positions 4*a* of rare earth metal atoms and 4*c* of *Ni* atoms (Fig. 1). In turn, the vacancies in the *RNiSb* crystal structure are point defects of an acceptor nature, which generate the corresponding acceptor states $\varepsilon_A^{Vac}$ in the band gap $\varepsilon_g$ [7]. Therefore, the nature of the hole-type conductivity of half-Heusler *RNiSb* phases is understandable, as indicated by the results of kinetic and galvanomagnetic studies [5 – 7].

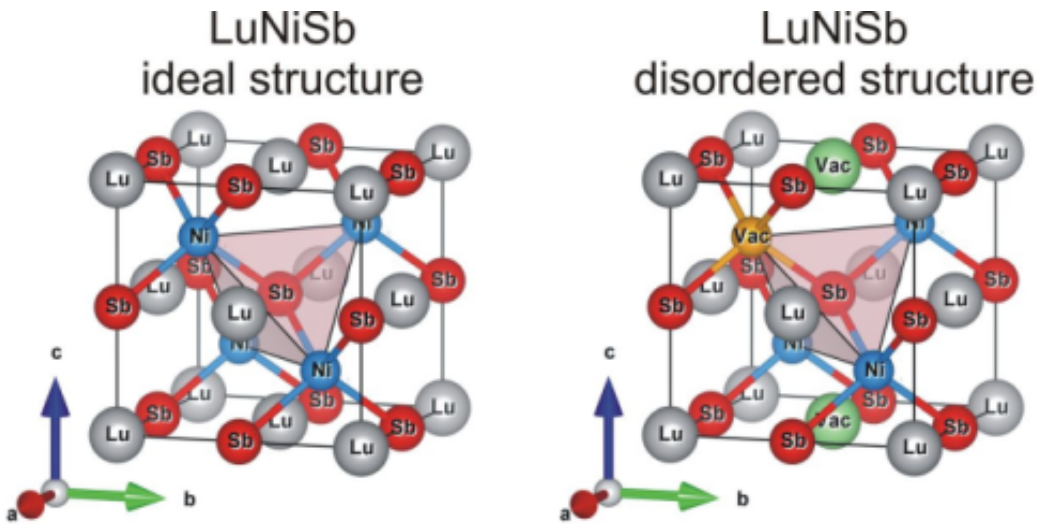


*Fig. 1. Models of the crystal structure of the half-Heusler phase of LuNiSb*

Previous studies of semiconductor thermoelectric materials obtained by doping *p-RNiSb* (*R – Er, Tm, Lu*) with *Zr* or *Sc* atoms by substituting rare earth metal atoms in the crystallographic position 4*a* [8 – 14] made it possible to understand the mechanisms of energy state generation. Thus, replacing *Er* ($5d^06s^2$) or *Lu* atoms with *Zr* ($4d^25s^2$) atoms or occupying the last vacancies in position 4*a* generates structural defects of the donor nature (*Zr* has more *d*-electrons than *Er* or *Lu*) [8 – 10]. At the same time, corresponding donor states appear in the $\varepsilon_g$ band gap of $Er_{1-x}Zr_xNiSb$ or $Lu_{1-x}Zr_xNiSb$ semiconductors. In the case of substitution of *R* atoms for *Sc* atoms in position 4*a* in semiconductors $Er_{1-x}Sc_xNiSb$, $Tm_{1-x}Sc_xNiSb$ and $Lu_{1-x}Sc_xNiSb$, defects of a neutral nature are generated (*Er*, *Tm*, *Lu* and Sc atoms are located in the same group of the Periodic System of Chemical Elements) [11 – 14]. However, when *Sc* atoms occupy vacancies in position 4*a* [7], defects of the acceptor nature and the corresponding acceptor states $\varepsilon_A^{Vac}$ disappear, and defects of the donor nature and donor states are generated. At the same time, at all concentrations of $Er_{1-x}Sc_xNiSb$, $Tm_{1-x}Sc_xNiSb$ and $Lu_{1-x}Sc_xNiSb$, holes remain current carriers, and the Fermi level $\varepsilon_F$ lies near the valence band $\varepsilon_V$.

The first step in the study of the new semiconductor thermoelectric material $Lu_{1-x}V_xNiSb$ is the modeling of its properties, which is the subject of this work. The difficulty of such modeling lies in the unpredictability of the behavior of *V* atoms. First, *V* atoms can be in different valence states (from +1 to +5). Secondly, when *V* atoms are introduced into the structure of the *LuNiSb* compound by substituting *Lu* atoms in the 4*a* position, they can occupy other crystallographic positions. After all, the atomic radius of *V* ($r_V$ = 0.134 nm) is much smaller than that of *Lu* ($r_{Lu}$ = 0.173 nm) and *Sb* ($r_{Sb}$ = 0.159 nm) and is close to the atomic radius of *Ni* (($r_{Ni}$ = 0.125 nm). Therefore, changes are possible in the structure of the semiconductor $Lu_{1-x}V_xNiSb$ associated with the occupation of different positions by *V* atoms. In particular, *V* atoms are able to occupy the 4*c* position by

occupying vacancies and/or replacing *Ni* atoms. The latter will lead to the generation of structural defects of an acceptor nature. The following results of modeling the properties of the semiconductor solid solution $Lu_{1-x}V_xNiSb$ will show the prospects of its use as an effective thermoelectric material.

## Research methods

Thermodynamic, structural, energy, and kinetic properties of the new semiconductor solid solution $Lu_{1-x}V_xNiSb$, obtained by doping the *p-LuNiSb* semiconductor by replacing *Lu* atoms with *V* atoms in the crystallographic position 4*a*, were simulated. DFT calculations were performed using the Vienna Ab initio Simulation Package VASP v. 5.4.4 [15] with potentials of the PAW type [16]. The exchange-correlation functional Perdew-Burke-Enzerhoff in the generalized gradient approximation (GGA) Monkhorst-Pack [17] for the *k*-grid 11 × 11 × 11 [18] was used. In all calculations, the plane wave cutoff was set to 400 eV. A supercell approach was used for mixed-arrangement crystal structures. In this case, lattice symmetry was reduced and all unique distributions of atoms were generated using a combinatorial approach [19]. The lattice parameters for such structures were optimized by a variable lattice volume, which was then selected by the universal equation of state [20]. The electronic kinetic coefficients were calculated using the Exciting code [21] (FLAPW - Full Potential Linearized Augmented Plane Waves method) by solving the linearized Boltzmann equation in the approximation of a constant relaxation time [22 – 25]. The modeling of the distribution of the density of electronic states (DOS) was carried out using the Korringa-Kohn-Rostoker (KKR) method (AkaiKKR software package [26]) in the Coherent Potential Approximation (CPA) and Local Density Approximation (LDA) for exchange correlation potential with the Moruzzi-Janak-Williams (MJW) parameterization [27]. The accuracy of calculating the position of the Fermi level $\varepsilon_F$ is ± 6 meV.

## Modeling of structural and thermodynamic properties of $Lu_{1-x}V_xNiSb$

Based on the assumption that there is a continuous solid solution of the substitution $Lu_{1-x}V_xNiSb$, $x$ = 0–1.0, the change in values of the unit cell period $a(x)$ for the ordered variant of the crystal structure was calculated (Fig. 2, curve 1). In this case, all crystallographic positions are occupied by atoms corresponding to the *MgAgAs* structural type [1], and *V* atoms replace *Lu* atoms in position 4*a*. Modeling the change in the period of the $Lu_{1-x}V_xNiSb$, $x$ = 0–1.0, shows a monotonous decrease in the values of a($x$) (Fig. 2, curve 1). The obtained result is logical, since the substitution of large *Lu* atoms ($r_{Lu}$ = 0.173 nm) with much smaller *V* atoms ($r_V$ = 0.134 nm) in position 4*a* should lead to a decrease in the period of the unit cell a($x$) $Lu_{1-x}V_xNiSb$. Such structural changes will lead to the formation of defects of a donor nature in the crystal structure of the semiconductor, and impurity donor states $\varepsilon_D^V$ will be generated in the band gap $\varepsilon_g$ $Lu_{1-x}V_xNiSb$ [28] (*V* has more *d*-electrons than *Lu*).

Modeling of thermodynamic characteristics in the approximation of harmonic oscillations of atoms for a hypothetical solid solution of $Lu_{1-x}V_xNiSb$, $x$ = 0–1.0, allows us to establish the energetic feasibility of the existence of such a substitution solid solution. For this purpose, a simulation of the

change in the values of the mixing enthalpy $\Delta H_{mix}(x)$ $Lu_{1-x}V_xNiSb$, $x$ = 0–1.0, was carried out (Fig., curve 2). The calculation shows the energetic expediency of the existence of a solid solution of substitution $Lu_{1-x}V_xNiSb$ only at concentrations $x$ = 0–0.10. This is evidenced by the low values of the mixing enthalpy $\Delta H_{mix}(x)$. At higher concentrations of $V$, $x$ > 0.10, delamination occurs (spinoid phase decay).

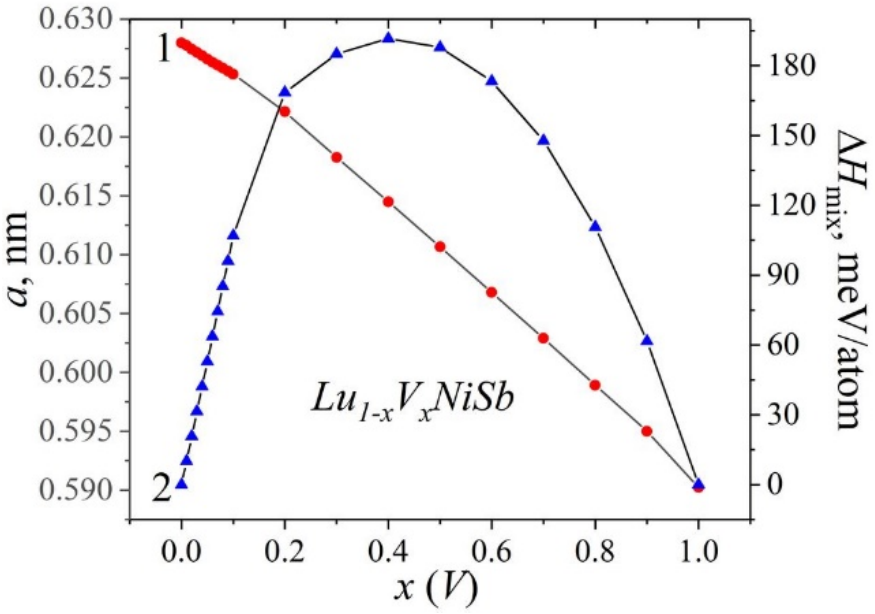


*Fig. 2. Modeling of changes in the values of the period of the elementary cell a(x) (1) and enthalpy of mixing $\Delta H_{mix}(x)$ (2) $Lu_{1-x}V_xNiSb$*

## Modeling of the electronic structure of $Lu_{1-x}V_xNiSb$

To predict the behavior of the Fermi level $\varepsilon_F$, the band gap $\varepsilon_g$, and the kinetic characteristics of $Lu_{1-x}V_xNiSb$, the distribution of the density of electronic states (DOS) was first calculated for two variants of the structure of the *LuNiSb* compound (Fig. 3). As can be seen from fig. 3, the simulation results are diametrically opposed. Thus, for the first, ordered version of the structure, when *V* atoms replace *Lu* atoms in position 4*a* (Fig. 3a), DOS simulation places the Fermi level $\varepsilon_F$ near the conduction band $\varepsilon_C$. This is typical for semiconductors of the electronic conductivity type [28]. In the case of a disordered version of the *LuNiSb* structure (Fig. 3b), when there are vacancies (Vac) in positions 4*a* of Lu atoms and 4*c* of *Ni* atoms (Fig. 1), the Fermi level $\varepsilon_F$ lies near the valence band $\varepsilon_V$. In this case, the DOS simulation corresponds to hole-type semiconductors [28].

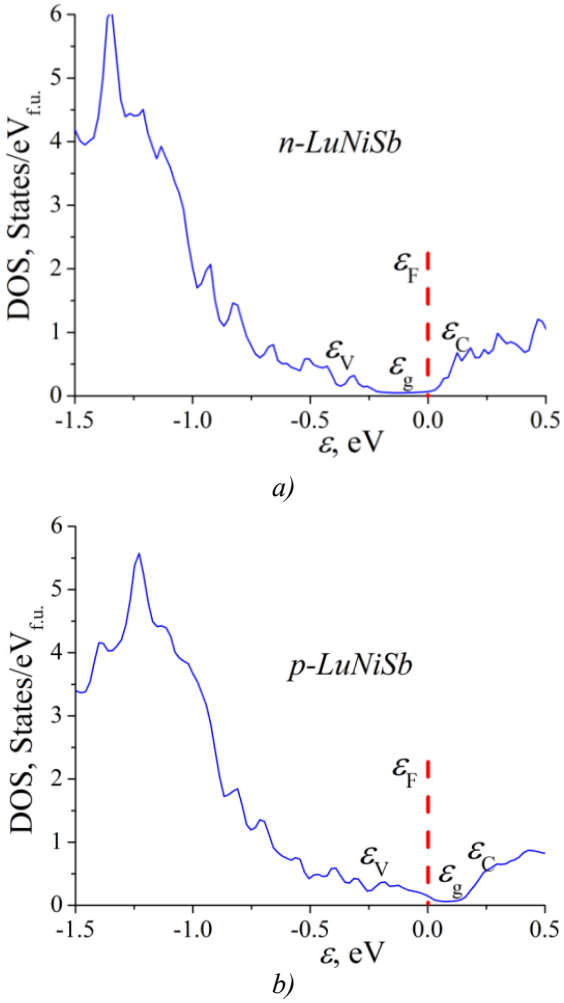


*Fig. 3. Calculation of the distribution of the DOS density of electronic states for the ordered (a) and disordered (b) versions of the structure of the LuNiSb compound*

Since the replacement of *Lu* atoms by *V* atoms generates structural defects of the donor nature, and in the band gap $\varepsilon_g$ of the semiconductor $Lu_{1-x}V_xNiSb$ near the conduction band $\varepsilon_C$, donor states $\varepsilon_D^V$ appear that form the donor band, then already at a $Lu_{0.99}V_{0.01}NiSb$ concentration, the Fermi level $\varepsilon_F$ will approach the edge of the conduction zone $\varepsilon_C$ (Fig. 4). At higher concentrations of *V* atoms, the concentration of donor states $\varepsilon_D^V$ and the strength of the donor zone will increase, and the Fermi level $\varepsilon_F$ will approach, and later cross the conduction band $\varepsilon_C$: a dielectric-metal conduction transition will occur, which is the Anderson transition [28]. The approach of the Fermi level $\varepsilon_F$ to the conduction band $\varepsilon_C$ will also lead to a change in the sign of the thermopower coefficient $\alpha(T, x)$ from positive (for *p-LuNiSb*) to negative, and electrons will become the main current carriers of $Lu_{1-x}V_xNiSb$. In addition, the intersection of the Fermi level $\varepsilon_F$ and the edge of the conduction band $\varepsilon_C$ will change the type of conductivity of the semiconductor from activation (for *p-LuNiSb*) to metallic [28]: in the experiment on the temperature dependences of the resistivity $\ln(\rho(1/T))$ $Lu_{1-x}V_xNiSb$ will disappear activation areas, and the resistance values $\rho$ will increase with temperature.

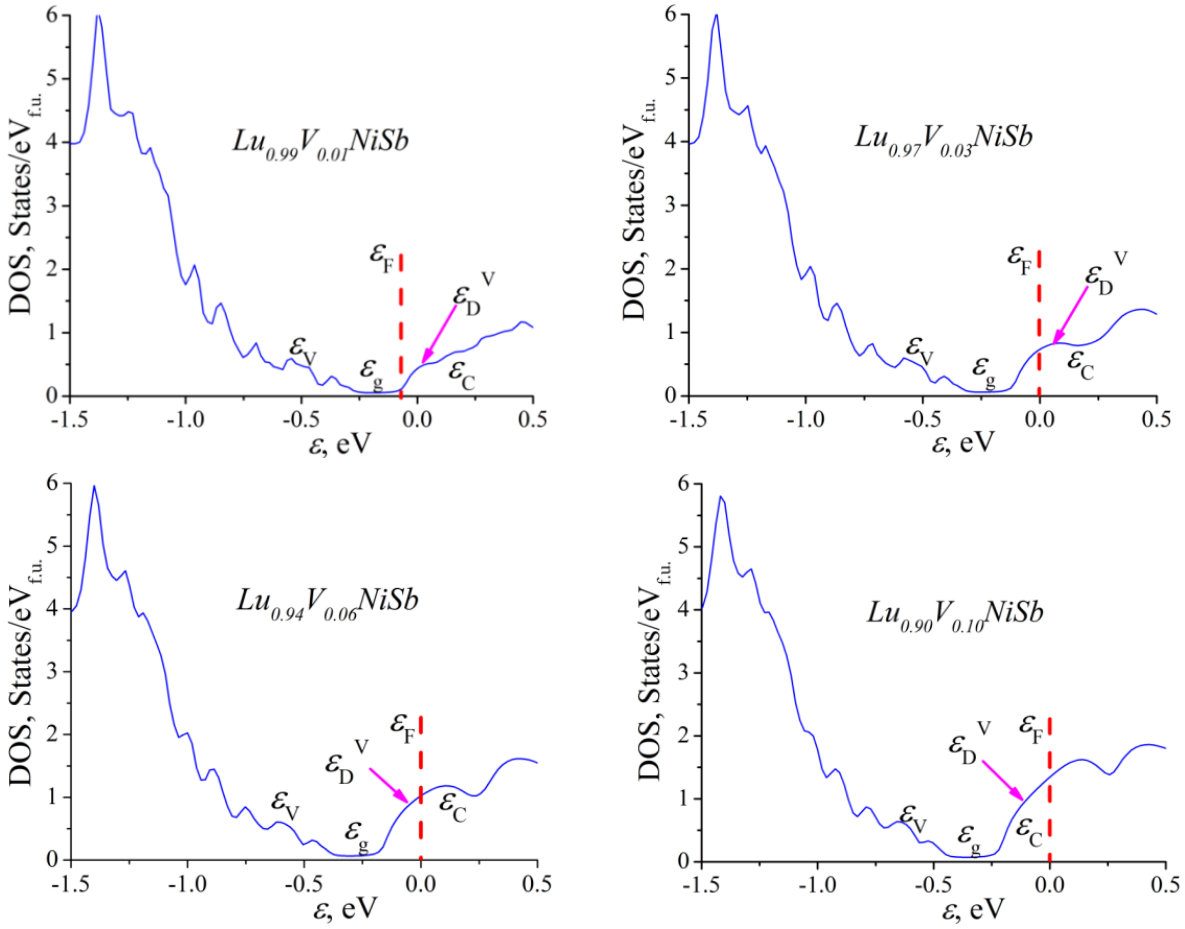


*Fig. 4. Calculation of the distribution of the density of electronic states of DOS $Lu_{1-x}V_xNiSb$*

## Modeling of the electrokinetic properties of $Lu_{1-x}V_xNiSb$

In fig. 5 shows the results of modeling the temperature dependences of the specific resistance $\rho(T, x)$ and the thermopower coefficient $\alpha(T,x)$ $Lu_{1-x}V_xNiSb$, $x \leq 0.10$. The result of calculating the temperature dependences of $\rho(T)$ and $\alpha(T)$ for *p-LuNiSb* coincides with that obtained earlier [2, 8, 9] and shows a decrease in the resistance values when holes are activated from the acceptor states $\varepsilon_A^{Vac}$ into the valence band $\varepsilon_V$. At the same time, the holes are the main carriers of the current, which is indicated by the positive values of the thermopower coefficient $\alpha(T)$. This behavior of electrical resistance $\rho(T)$ is characteristic of semiconductors, when the number of free current carriers increases due to their thermal activation from the Fermi level $\varepsilon_F$ to the continuous energy zone [28].

Doping *p-LuNiSb* with *V* atoms by substituting *Lu* atoms in the 4*a* position generates structural defects of a donor nature in the semiconductor $Lu_{1-x}V_xNiSb$, and corresponding donor states $\varepsilon_D^V$ appear in the $\varepsilon_g$ band gap. As can be seen from fig. 5, at the lowest impurity concentration ($x = 0.01$) in the temperature range $T = 10$–$170$ K, the values of specific electrical resistance $\rho(T)$ in the semiconductor $Lu_{0.99}V_{0.01}NiSb$ increase. At the same time, the main current carriers, as in the case of *p-LuNiSb*, are holes, as indicated by the positive values of the thermopower coefficient $\alpha(T)$.

Such an increase in the values of electrical resistance ρ(*T*) is not a manifestation of metallic conductivity, when the increase in resistance is associated with the action of current carrier scattering mechanisms. In the case of the semiconductor $Lu_{0.99}V_{0.01}NiSb$, the increase in the values of specific electrical resistance ρ(*T*) at temperatures *T* = 10–170 K is of a concentration nature. After all, the basic semiconductor *p-LuNiSb* contains acceptor states $\varepsilon_A^{Vac}$, which in $Lu_{0.99}V_{0.01}NiSb$ with increasing temperature capture electrons from the generated donor states $\varepsilon_D^V$, which reduces the concentration of free holes and increases the degree of compensation and the value of electrical resistance ρ(*T*). At the same time, the Fermi level $\varepsilon_F$ drifts from the edge of the valence band $\varepsilon_V$ to the middle of the band gap $\varepsilon_g$, which it will cross at a temperature of $T \approx 65$ K. At higher temperatures, $T > 65$ K, the sign of the thermopower coefficient α(*T*) $Lu_{0.99}V_{0.01}NiSb$ becomes negative, the Fermi level $\varepsilon_F$ now drifts to the conduction band $\varepsilon_C$. The extremum on the dependence of the specific resistance ρ(*T*) of $Lu_{0.99}V_{0.01}NiSb$ at a temperature of $T \approx 170$ K and the subsequent decrease in the electrical resistance values (Fig. 5, inset) is also of a concentration nature. All acceptor states are compensated, but the Fermi level $\varepsilon_F$ lies in the band gap $\varepsilon_g$ near the edge of the conduction band $\varepsilon_C$ and the concentration of free electrons increases during the ionization of donor states $\varepsilon_D^V$.

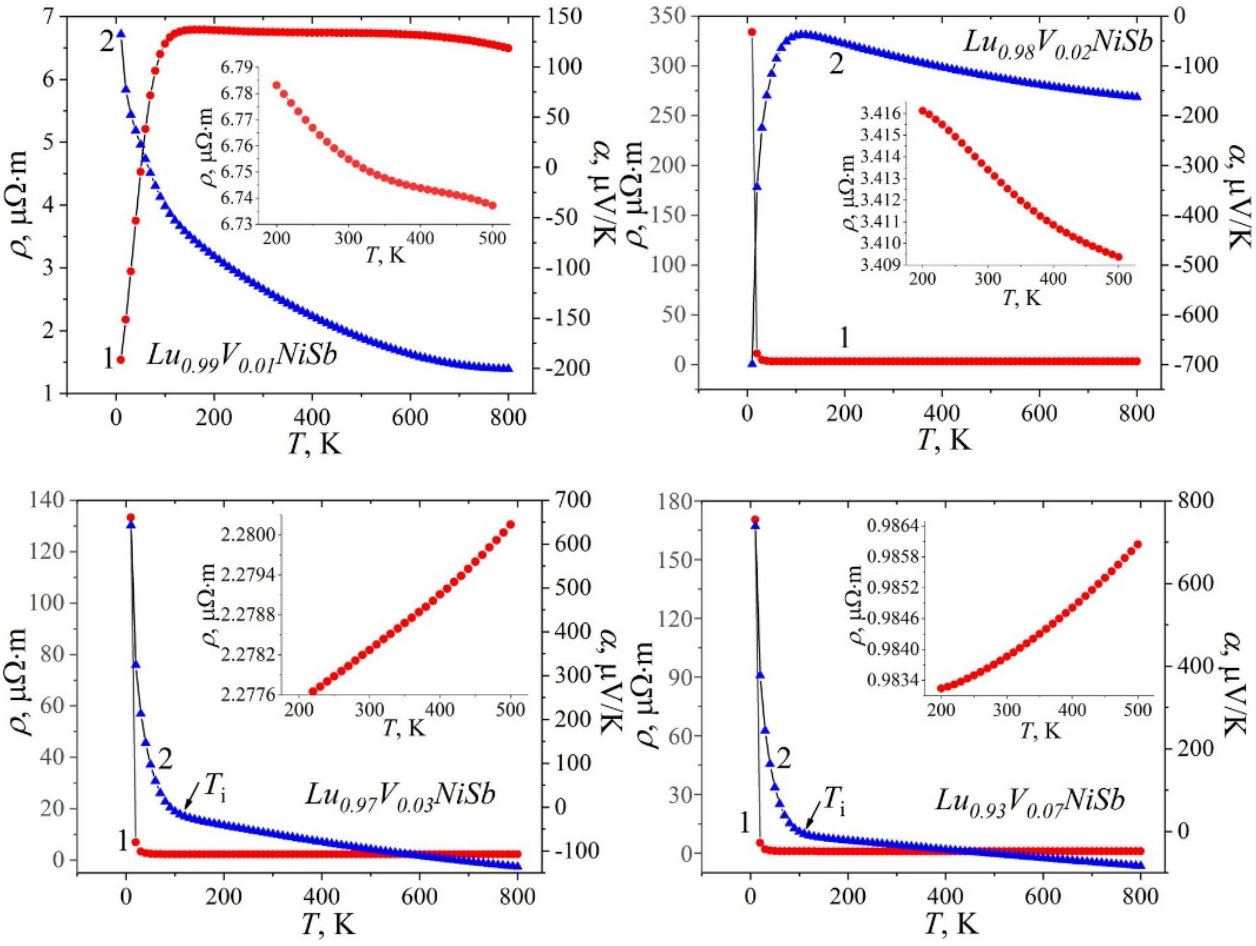


*Fig. 5. Modeling of the change in the values of specific electrical resistance ρ(T,x) (1) and thermopower coefficient α(T,x) (2) $Lu_{1-x}V_xNiSb$*

In the $Lu_{0.98}V_{0.02}NiSb$ semiconductor, the temperature dependence of the specific resistance $\rho(T, x)$ at low temperatures does not include the region of increase in resistance values, which was in $Lu_{0.99}V_{0.01}NiSb$ and is associated with a decrease in the concentration of holes during the compensation of the acceptor states $\varepsilon_A^{Vac}$ by electrons of ionized donor states $\varepsilon_D^V$. The simulation shows only a rapid decrease in the values of the specific resistance $\rho(T, x)$ from $\rho_{10\ K} = 333.7$ μΩ·m to the values $\rho_{20\ K} = 11.2$ μΩ·m and $\rho_{30\ K} = 4.9$ μΩ·m. At the same time, the sign of the thermopower coefficient $\alpha(T, x)$ $Lu_{0.98}V_{0.02}NiSb$ remains negative at all the investigated temperatures. This behavior of the temperature dependences $\rho(T, x)$ and $\alpha(T, x)$ of $Lu_{0.98}V_{0.02}NiSb$ indicates that all acceptor states $\varepsilon_A^{Vac}$ are compensated, the Fermi level $\varepsilon_F$ is fixed at the donor states $\varepsilon_D^V$ and is in the band gap $\varepsilon_g$ near the edge conduction zones $\varepsilon_C$.

The results of modeling the kinetic characteristics of $Lu_{1-x}V_xNiSb$ at higher concentrations of the impurity $V$, $x \geq 0.03$, indicate the appearance of a significant number of structural defects of an acceptor nature in the semiconductor. This is evidenced by the positive values of the thermopower coefficient $\alpha(T, x)$ at temperatures $T \leq 90$ K in the semiconductor $Lu_{0.97}V_{0.03}NiSb$ and $T \leq 100$ K in the semiconductor $Lu_{0.93}V_{0.07}NiSb$ (Fig. 5). We noted above that $V$ atoms ($3d^34s^2$) can occupy different crystallographic positions in $Lu_{1-x}V_xNiSb$, in particular, the 4*c* position of *Ni* atoms ($3d^84s^2$). The latter will lead to the generation of structural defects of an acceptor nature ($V$ has fewer 3*d*-electrons than *Ni*) and the appearance of impurity acceptor states $\varepsilon_A^{Ni}$ in the band gap. At these temperatures, holes are the main current carriers.

At higher temperatures $T > T_i$, the sign of the thermopower coefficient $\alpha(T, x)$ is inverted from positive to negative (Fig. 5), and electrons become the main current carriers. The fact that the inversion of the sign of the thermopower coefficient $\alpha(T, x)$ occurs at temperatures $T_i > 90$–100 K indicates that in the band gap $\varepsilon_g$ of a semiconductor, the depth of donor states $\varepsilon_D^V$ relative to the edge of the conduction band $\varepsilon_C$ is greater than that of acceptor states of $\varepsilon_A^{Ni}$ states relative to the valence band edge $\varepsilon_V$. Therefore, at low temperatures, acceptors are first ionized, and at higher temperatures, $T > T_i$, donors are ionized. Such a change in the sign of the thermopower coefficient $\alpha(T, x)$ $Lu_{1-x}V_xNiSb$ (of the type of main current carriers) shows that at concentrations of $V$ atoms, $x \geq 0.03$, the number of structural defects of the donor nature outweighs the number of defects of the acceptor nature.

Modeling the temperature dependences of the specific electrical resistance $\rho(T, x)$ $Lu_{1-x}V_xNiSb$, $x \geq 0.03$, shows that in the semiconductor $Lu_{0.97}V_{0.03}NiSb$, the resistance values decrease in the temperature range $T = 10$–160 K, and only increase at higher temperatures (Fig. 5, inset). In the case of the semiconductor $Lu_{0.93}V_{0.07}NiSb$, a decrease in the values of the specific resistance $\rho(T, x)$ occurs at temperatures $T = 10$–110 K, after which the resistance increases. This behavior $\rho(T, x)$ $Lu_{1-x}V_xNiSb$, $x \geq 0.03$, shows that at low temperatures the Fermi level $\varepsilon_F$ is in the band gap $\varepsilon_g$ of the semiconductor, and at higher temperatures it crosses the edge of the conduction band $\varepsilon_C$ and moves along the band of continuous energies. A dielectric-metal conduction transition will occur, which is an Anderson transition [28]. In the case of experimental measurements on the temperature dependence of the

specific electrical resistance ln(ρ(1/*T*)) $Lu_{1-x}V_xNiSb$, there will be no high-temperature activation areas, and the resistance values ρ will increase with temperature.

## Modeling of thermoelectric characteristics of $Lu_{1-x}V_xNiSb$

An exhaustive characteristic of a thermoelectric material in terms of its efficiency in converting thermal energy into electrical energy is the value of the thermoelectric factor at different temperatures. In fig. 6 shows the results of *ZT* modeling in the temperature range $T = 10–800$ K for the semiconductor solid solution $Lu_{1-x}V_xNiSb$, $x \leq 0.10$. Note that the electronic component of thermal conductivity $\kappa_e$ was taken into account when modeling the values of the thermoelectric factor *Z*.

From fig. 6, we can see that in the semiconductor solid solution $Lu_{0.99}V_{0.01}NiSb$ at a temperature of $T \approx 620$ K, the thermoelectric factor *Z* are maximal and reach the values of $ZT = 0.62$. The values of the thermoelectric factor obtained by mathematical modeling for $Lu_{1-x}V_xNiSb$, $x \leq 0.10$, testify to the prospects of the obtained semiconductor solid solution as a thermoelectric material.

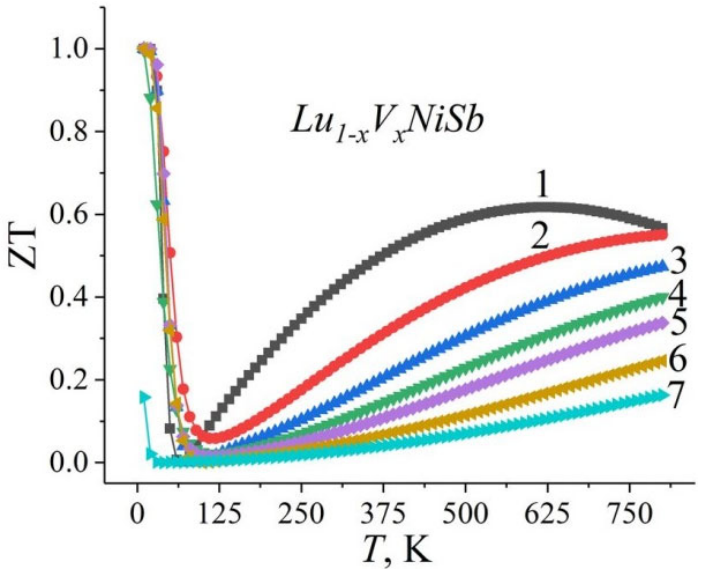


*Fig. 6. Modeling the change in ZT values of $Lu_{1-x}V_xNiSb$ with increasing temperature:*
*1 – x = 0.01; 2 – x = 0.02; 3 – x = 0.03; 4 – x = 0.04;*
*5 – x = 0.05; 6 – x = 0.07; 7 – x = 0.10*

## Conclusion

The result of modeling the crystal and electronic structures, thermodynamic and kinetic properties of $Lu_{1-x}V_xNiSb$ is establishing the nature of the generated energy states. It is shown that the semiconductor solid solution $Lu_{1-x}V_xNiSb$ is a promising thermoelectric material, and at a temperature of $T \approx 620$ K and a concentration of $Lu_{0.99}V_{0.01}NiSb$, the thermoelectric factor *Z* values reach the maximum values of $ZT = 0.62$. It was established that the impurity atoms of *V* ($3d^3 4s^2$), introduced

into the structure of the *LuNiSb* compound, simultaneously occupy the crystallographic positions 4*a* of *Lu* atoms ($5d^16s^2$) and 4*c* of *Ni* atoms ($3d^84s^2$) in different ratios, generating in the band gap $\varepsilon_g$ impurity donor $\varepsilon_D^V$ and acceptor $\varepsilon_A^{Ni}$ energy states. The ratio of concentrations of donors and acceptors determines the location of the Fermi level $\varepsilon_F$ and the mechanisms of electrical conductivity.

## References

1. Romaka V. V., Rogl P. F., Carlini R., Fanciulli C. (2017). Prediction of the Thermoelectric Properties of Half-Heusler Phases from the Density Functional Theory. – P. 286 - 323. In "*Alloys and Intermetallic Compounds. From Modeling to Engineering*". Genova, Italy: CRC Press Taylor & Francis Group. International Standard Book Number–13: 978–1–4987–4143–9.
2. Romaka V. A., Stadnyk Yu. V., Krayovskyy V. Ya., Romaka L. P., Guk O. P., Romaka V. V., Mykyuchuk M. M., Horyn A. M. (2020). *Novitni termochutlyvi materialy ta peretvoriuvachi temperatury* [*New thermosensitive materials and temperature converters*]. Lviv: Lvivska Polytechnika [in Ukrainian]. DOI: https://opac.lpnu.ua/bib/1131184.
3. Hartjes K., Jeitschko W. (1995). Crystal structure and magnetic properties of the lanthanoid nickel antimonides *LnNiSb* (*Ln = La–Nd, Sm, Gd–Tm, Lu*). *J. Alloys Compd*., 226, 81-86. DOI: https://doi.org/10.1016/0925-8388(95)01573-6.
4. Anatychuk L. I. (1979). *Termoelementy i termoelectricheskiie ustroistva. Spravochnik.* [*Thermoelements and thermoelectric devices. Reference book*]. Kyiv: Naukova dumka [in Russian].
5. Karla I., Pierre J., Skolozdra R. V. (1998). Physical properties and giant magnetoresistance in R*NiSb* compounds. *J. Alloys Compd*., 265, 42 - 48. DOI: https://doi.org/10.1016/S0925-8388(97)00419-2.
6. Romaka V. V., Romaka L., Horyn A., Rogl P., Stadnyk Yu., Melnychenko N., Orlovskyy M., Krayovskyy V. (2016). Peculiarities of thermoelectric half-Heusler phase formation in *Gd-Ni-Sb* and *Lu-Ni-Sb* ternary systems. *J. Solid State Chem*., 239, 145 - 152. https://doi.org/10.1016/j.jssc.2016.04.029).
7. Romaka V.V., Romaka L., Horyn A., Stadnyk Yu. (2021). Experimental and theoretical investigation of the *Y–Ni–Sb* and *Tm–Ni–Sb* systems. *J. Alloys Compd*., 855, 157334–12. DOI: https://doi.org/10.1016/j.jallcom.2020.157334.
8. Romaka V. A., Stadnyk Yu. V., Romaka L. P., Pashkevych V. Z., Romaka V. V., Horyn A. M., Demchenko P. Yu. (2021). Study of structural, thermodynamic, energy, kinetic and magnetic properties of thermoelectric material $Lu_{1-x}Zr_xNiSb$. *J. Thermoelectricity*, 1, 32 - 48. DOI: http://jt.inst.cv.ua/jt/jt_2021_01_en.pdf.
9. Romaka V. A., Stadnyk Yu., Romaka L., Horyn A., Pashkevych V., Nychyporuk H., Garanyuk P. (2022). Investigation of Thermoelectric Material Based on $Lu_{1-x}Zr_xNiSb$ Solid Solution. I. Experimental Results. *J. Phys. Chem. Sol. State*, 23, 235-241. DOI: 10.15330/pcss.23.2.235-241.
10. Romaka V. A., Stadnyk Yu., Romaka L., Krayovskyy V., Horyn A., Klyzub P., Pashkevych V. (2020). Study of structural, electrokinetic and magnetic characteristics of the $Er_{1-x}Zr_xNiSb$ Semiconductor. *J. Phys. Chem. Sol. State*, 21, 689-694. DOI: 10.15330/pcss.21.4.689-694.

11. Wolańska I., Synoradzki K., Ciesielski K., Załęski K., Skokowski P., Kaczorowski D. (2019). Enhanced thermoelectric power factor of half-Heusler solid solution *$Sc_{1-x}Tm_xNiSb$* prepared by high-pressure hightemperature sintering method. *Materials Chemistry and Physics*, 227, 29 - 35. DOI: https://doi.org/10.1016/j.matchemphys.2019.01.056.
12. Romaka V. V., Romaka V. A., Stadnyk Yu. V., Romaka L. P., Demchenko P. Y., Pashkevych V. Z., Horyn A. M. (2022). Features of mechanisms of electrical conductivity in semiconductive solid solution *$Lu_{1-x}Sc_xNiSb$*. *Ukr. J. Phys*., 67, 370-379. DOI: https://doi.org/10.15407/ujpe67.5.370.
13. Romaka V. A., Stadnyk Yu. V., Romaka V. V., Demchenko P. Yu., Romaka L. P., Pashkevych V. Z., Horyn A. M., Horpeniuk A. Ya. (2021). Investigation of properties of new thermoelectric material *$Lu_{1-x}Sc_xNiSb$*. *J. Thermoelectricity*, 2, 18 - 30. DOI: http://jt.inst.cv.ua/jt/jt_2021_02_en.pdf.
14. Romaka V. A., Stadnyk Yu., Romaka L., Krayovskyy V., Klyzub P., Pashkevych V., Horyn A., Garanyuk P. (2021). Synthesis and Electrical Transport Properties of *$Er_{1-x}Sc_xNiSb$* Semiconducting Solid Solution. *J. Phys. Chem. Sol. State*, 22, 146–152. DOI:10.15330/pcss.22.1.146-152.
15. Kresse G., Hafner J. (1993). Ab initio molecular dynamics for liquid metals. *Phys. Rev*., B 47, 558 - 561.
16. Kresse G., Joubert D. (1999). From ultrasoft pseudopotentials to the projector augmented-wave method. *Phys. Rev*., B 59, 1758 - 1775.
17. Perdew J. P., Burke K., Ernzerhof M. (1976). Generalized gradient approximation made simple. *Phys. Rev. Lett*., 77(18), 3865–8. https://doi.org/10.1103/PhysRevLett.77.3865.
18. Monkhorst H. J., Pack J. K. (1976). Special points for Brillouin-zone integrations. *Phys. Rev*., B 13, 5188 - 5192.
19. Okhotnikov K., Charpentier T., Cadars S. (2016). Supercell program: a combinatorial structure-generation approach for the local-level modeling of atomic substitutions and partial occupancies in crystals. J. Cheminform, 8(17), 1 - 15.
20. Vinet P., Rose J. H., Jr Ferrante J. S. (1989). Universal features of the equation of state of solids. *J. Phys.: Condens. Matter*., 1, 1941 - 1964.
21. Gulans A., Kontur S., Meisenbichler C., Nabok D., Pavone P., Rigamonti S., Sagmeister S., Werner U., Draxl C. (2014). Exciting – a full-potential all-electron package implementing density-functional theory and many-body perturbation theory. *J. Phys.: Condens Matter*., 26, 363202, 1 - 24.
22. Nag B. R. (1996). *Electron Transport in Compound Semiconductors*. Berlin: Springer Verlag.
23. Mahan G. D. and Sofo J. O. (1996). The best thermoelectric. *Proc. Natl. Acad. Sci. USA*, 93 7436.
24. Scheidemantel T. J., Ambrosch-Draxl C., Thonhauser T., Badding H. V., and Sofo J. O. (2003). Transport coefficients from first-principles calculations. *Phys. Rev*., B 68, 125210.
25. Babak V. P., Babak S. V., Myslovych M. V., Zaporozhets A. O., Zvaritch V. M. (2020). Technical provision of diagnostic systems. *Studies in Systems, Decision and Control*, 281, 91 - 133. https://doi.org/10.1007/978-3-030-44443-3_4
26 Schruter M., Ebert H., Akai H., Entel P., Hoffmann E., Reddy G. G. (1995). First-principles investigations of atomic disorder effects on magnetic and structural instabilities in transition-

metal alloys. *Phys. Rev*. B 52, 188 - 209

27 Moruzzi V. L., Janak J. F., Williams A. R. (1978). *Calculated Electronic Properties of Metals*. NY: Pergamon Press.

28 Shklovskii B. I. and Efros A. L. (1984). *Electronic properties of doped semiconductors*. Berlin, Heidelberg, Springer-Verlag. DOI: 10.1007/978-3-662-02403-4.

Submitted 15.02.2022

**Ромака В. А.,** *док. техн. наук*, *канд. фіз.-мат., професор* [1]
**Стадник Ю. В,** *канд. хім. наук*[2]
**Ромака Л. П.** *канд. хім. наук*[2]
**Плевачук Ю. О.** *док. фіз.-мат.*[2]
**Ромака В. В.** *док. техн. наук*, *канд. хім. наук*[3]
**Горинь А. М.** *канд. хім. наук*[2]
**Пашкевич В. З.** *канд. тех. наук*[1]**,**
**Зелінський А. В.** *канд. хім. наук*[2]

[1]Національний університет "Львівська політехніка",
вул. С. Бандери, 12, Львів, 79013, Україна;
[2]Львівський національний університет ім. І. Франка,
вул. Кирила і Мефодія, 6, Львів, 79005, Україна;
[3]Інститут дослідження твердого тіла ім. Лейбніца, Гельмгольц штрасе,
20, 01069 Дрезден, Німеччина

## ДОСЛІДЖЕННЯ ТЕРМОЕЛЕКТРИЧНОГО МАТЕРІАЛУ $Lu_{1-x}V_xNiSb$: МОДЕЛЮВАННЯ ВЛАСТИВОСТЕЙ

*Результатом моделювання кристалічної та електронної структур, термодинамічних та кінетичних властивостей $Lu_{1-x}V_xNiSb$ є встановлення природи генерованих енергетичних станів. Показано, що напівпровідниковий твердий розчин $Lu_{1-x}V_xNiSb$ є перспективним термоелектричним матеріалом, а за температури T≈620 K та концентрації $Lu_{0.99}V_{0.01}NiSb$ значення добротності досягають максимальних значень ZT = 0.62. Встановлено, що домішкові атоми V ($3d^34s^2$), уведені до структури сполуки LuNiSb, одночасно у різних співвідношеннях займають кристалографічні позиції 4a атомів Lu ($5d^16s^2$) та 4c атомів Ni*

*($3d^8 4s^2$), генеруючи в забороненій зоні $\varepsilon_g$ домішкові донорні $\varepsilon_D^V$ та акцепторні $\varepsilon_A^{Ni}$ енергетичні стани. Співвідношення концентрацій донорів та акцепторів визначає розташування рівня Фермі $\varepsilon_F$ та механізми електропровідності. Бібл. 28, рис.6.*

**Ключові слова**: електронна структура, термоелектрична добротність, електроопір, коефіцієнт термоЕРС.

## References

1. Romaka V. V., Rogl P. F., Carlini R., Fanciulli C. (2017). Prediction of the Thermoelectric Properties of Half-Heusler Phases from the Density Functional Theory. – P. 286 - 323. In "*Alloys and Intermetallic Compounds. From Modeling to Engineering*". Genova, Italy: CRC Press Taylor & Francis Group. International Standard Book Number–13: 978–1–4987–4143–9.
2. Romaka V. A., Stadnyk Yu. V., Krayovskyy V. Ya., Romaka L. P., Guk O. P., Romaka V. V., Mykyuchuk M. M., Horyn A. M. (2020). *Novitni termochutlyvi materialy ta peretvoriuvachi temperatury* [*New thermosensitive materials and temperature converters*]. Lviv: Lvivska Polytechnika [in Ukrainian]. DOI: https://opac.lpnu.ua/bib/1131184.
3. Hartjes K., Jeitschko W. (1995). Crystal structure and magnetic properties of the lanthanoid nickel antimonides *LnNiSb* (*Ln = La–Nd, Sm, Gd–Tm, Lu*). *J. Alloys Compd*., 226, 81-86. DOI: https://doi.org/10.1016/0925-8388(95)01573-6.
4. Anatychuk L. I. (1979). *Termoelementy i termoelectricheskiie ustroistva. Spravochnik*. [*Thermoelements and thermoelectric devices. Reference book*]. Kyiv: Naukova dumka [in Russian].
5. Karla I., Pierre J., Skolozdra R. V. (1998). Physical properties and giant magnetoresistance in R*NiSb* compounds. *J. Alloys Compd*., 265, 42 - 48. DOI: https://doi.org/10.1016/S0925-8388(97)00419-2.
6. Romaka V. V., Romaka L., Horyn A., Rogl P., Stadnyk Yu., Melnychenko N., Orlovskyy M., Krayovskyy V. (2016). Peculiarities of thermoelectric half-Heusler phase formation in *Gd-Ni-Sb* and *Lu-Ni-Sb* ternary systems. *J. Solid State Chem*., 239, 145 - 152. https://doi.org/10.1016/j.jssc.2016.04.029).
7. Romaka V.V., Romaka L., Horyn A., Stadnyk Yu. (2021). Experimental and theoretical investigation of the *Y–Ni–Sb* and *Tm–Ni–Sb* systems. *J. Alloys Compd*., 855, 157334–12. DOI: https://doi.org/10.1016/j.jallcom.2020.157334.
8. Romaka V. A., Stadnyk Yu. V., Romaka L. P., Pashkevych V. Z., Romaka V. V., Horyn A. M., Demchenko P. Yu. (2021). Study of structural, thermodynamic, energy, kinetic and magnetic properties of thermoelectric material $Lu_{1-x}Zr_xNiSb$. *J. Thermoelectricity*, 1, 32 - 48. DOI: http://jt.inst.cv.ua/jt/jt_2021_01_en.pdf.
9. Romaka V. A., Stadnyk Yu., Romaka L., Horyn A., Pashkevych V., Nychyporuk H., Garanyuk P. (2022). Investigation of Thermoelectric Material Based on $Lu_{1-x}Zr_xNiSb$ Solid Solution. I. Experimental Results. *J. Phys. Chem. Sol. State*, 23, 235-241. DOI: 10.15330/pcss.23.2.235-241.
10. Romaka V. A., Stadnyk Yu., Romaka L., Krayovskyy V., Horyn A., Klyzub P., Pashkevych V. (2020). Study of structural, electrokinetic and magnetic characteristics of the $Er_{1-x}Zr_xNiSb$ Semiconductor. *J. Phys. Chem. Sol. State*, 21, 689-694. DOI: 10.15330/pcss.21.4.689-694.

11. Wolańska I., Synoradzki K., Ciesielski K., Załęski K., Skokowski P., Kaczorowski D. (2019). Enhanced thermoelectric power factor of half-Heusler solid solution $Sc_{1-x}Tm_xNiSb$ prepared by high-pressure hightemperature sintering method. *Materials Chemistry and Physics*, 227, 29 - 35. DOI: https://doi.org/10.1016/j.matchemphys.2019.01.056.
12. Romaka V. V., Romaka V. A., Stadnyk Yu. V., Romaka L. P., Demchenko P. Y., Pashkevych V. Z., Horyn A. M. (2022). Features of mechanisms of electrical conductivity in semiconductive solid solution $Lu_{1-x}Sc_xNiSb$. *Ukr. J. Phys*., 67, 370-379. DOI: https://doi.org/10.15407/ujpe67.5.370.
13. Romaka V. A., Stadnyk Yu. V., Romaka V. V., Demchenko P. Yu., Romaka L. P., Pashkevych V. Z., Horyn A. M., Horpeniuk A. Ya. (2021). Investigation of properties of new thermoelectric material $Lu_{1-x}Sc_xNiSb$. *J. Thermoelectricity*, 2, 18 - 30. DOI: http://jt.inst.cv.ua/jt/jt_2021_02_en.pdf.
14. Romaka V. A., Stadnyk Yu., Romaka L., Krayovskyy V., Klyzub P., Pashkevych V., Horyn A., Garanyuk P. (2021). Synthesis and Electrical Transport Properties of $Er_{1-x}Sc_xNiSb$ Semiconducting Solid Solution. *J. Phys. Chem. Sol. State*, 22, 146–152. DOI:10.15330/pcss.22.1.146-152.
15. Kresse G., Hafner J. (1993). Ab initio molecular dynamics for liquid metals. *Phys. Rev*., B 47, 558 - 561.
16. Kresse G., Joubert D. (1999). From ultrasoft pseudopotentials to the projector augmented-wave method. *Phys. Rev*., B 59, 1758 - 1775.
17. Perdew J. P., Burke K., Ernzerhof M. (1976). Generalized gradient approximation made simple. *Phys. Rev. Lett*., 77(18), 3865–8. https://doi.org/10.1103/PhysRevLett.77.3865.
18. Monkhorst H. J., Pack J. K. (1976). Special points for Brillouin-zone integrations. *Phys. Rev*., B 13, 5188 - 5192.
19. Okhotnikov K., Charpentier T., Cadars S. (2016). Supercell program: a combinatorial structure-generation approach for the local-level modeling of atomic substitutions and partial occupancies in crystals. J. Cheminform, 8(17), 1 - 15.
20. Vinet P., Rose J. H., Jr Ferrante J. S. (1989). Universal features of the equation of state of solids. *J. Phys.: Condens. Matter*., 1, 1941 - 1964.
21. Gulans A., Kontur S., Meisenbichler C., Nabok D., Pavone P., Rigamonti S., Sagmeister S., Werner U., Draxl C. (2014). Exciting – a full-potential all-electron package implementing density-functional theory and many-body perturbation theory. *J. Phys.: Condens Matter*., 26, 363202, 1 - 24.
22. Nag B. R. (1996). *Electron Transport in Compound Semiconductors*. Berlin: Springer Verlag.
23. Mahan G. D. and Sofo J. O. (1996). The best thermoelectric. *Proc. Natl. Acad. Sci. USA*, 93 7436.
24. Scheidemantel T. J., Ambrosch-Draxl C., Thonhauser T., Badding H. V., and Sofo J. O. (2003). Transport coefficients from first-principles calculations. *Phys. Rev*., B 68, 125210.
25. Babak V. P., Babak S. V., Myslovych M. V., Zaporozhets A. O., Zvaritch V. M. (2020). Technical provision of diagnostic systems. *Studies in Systems, Decision and Control*, 281, 91 - 133. https://doi.org/10.1007/978-3-030-44443-3_4
26. Schruter M., Ebert H., Akai H., Entel P., Hoffmann E., Reddy G. G. (1995). First-principles investigations of atomic disorder effects on magnetic and structural instabilities in transition-metal alloys. *Phys. Rev*. B 52, 188 - 209

27. Moruzzi V. L., Janak J. F., Williams A. R. (1978). *Calculated Electronic Properties of Metals*. NY: Pergamon Press.
28. Shklovskii B. I. and Efros A. L. (1984). *Electronic properties of doped semiconductors*. Berlin, Heidelberg, Springer-Verlag. DOI: 10.1007/978-3-662-02403-4.

Submitted 15.02.2022